



# Phase transition in $[\text{Ca}(\text{NH}_3)_6](\text{ClO}_4)_2$ studied by neutron scattering methods and far infrared spectroscopy

Joanna Hetmańczyk<sup>a</sup>, Łukasz Hetmańczyk<sup>a,\*</sup>, Anna Migdał-Mikuli<sup>a</sup>, Edward Mikuli<sup>a</sup>, Ireneusz Natkaniec<sup>b,c</sup>

<sup>a</sup> Jagiellonian University, Faculty of Chemistry, Department of Chemical Physics, Phase Transitions Research Team, Ingardena 3, 30-060 Kraków, Poland

<sup>b</sup> Frank Laboratory of Neutron Physics, JINR, Dubna 141980, Russia

<sup>c</sup> H. Niewodniczański Institute of Nuclear Physics, PAS, Radzikowskiego 152, 31-342 Kraków, Poland

## ARTICLE INFO

### Article history:

Received 21 December 2010

Received in revised form 14 March 2011

Accepted 19 March 2011

Available online 27 March 2011

### Keywords:

Hexaamminecalcium chlorate(VII)

Phase transitions

Molecular reorientations

Fourier transform far infrared spectroscopy

(FT-FIR)

Inelastic and quasi-elastic incoherent neutron scattering (IINS and QENS) with simultaneous neutron powder diffraction (NPD)

## ABSTRACT

The results of inelastic and quasi-elastic incoherent neutron scattering with simultaneous neutron powder diffraction and of Fourier transform far infrared spectroscopy measurements carried out for  $[\text{Ca}(\text{NH}_3)_6](\text{ClO}_4)_2$  between 20–220 K and 8.5–295 K, respectively, are reported. The far infrared spectrum on cooling the substance indicates splitting of some degenerated vibrational modes, which suggests lowering of the crystal structure at the phase transition temperature  $T_C^c = 122.0$  K, revealed by us earlier using differential scanning calorimetry. In turn, lack of simultaneous abrupt narrowing of some broad infrared bands suggests an existence of fast molecular reorientational motions, which do not change their character in the wide temperature range. On the other hand, the quasi-elastic neutron scattering peak registered at 110 K and also at higher temperatures, shows distinct broadening, which is typical for dynamically, orientationally disordered crystals (ODIC). Reorientational motion of  $\text{NH}_3$  ligands can be well described by a model of instantaneous  $120^\circ$  jumps of protons around the 3-fold axis of Ca–N bonds, with the reorientational correlation time  $\tau_R$  of an order of picoseconds. However, the  $\text{NH}_3$  ligands did not drastically change either their jump rate or a character of their reorientational motions at the phase transition temperature ( $T_C$ ). The estimated mean value of activation energy for  $\text{NH}_3$  ligands reorientation in both phases  $E_a = 1.2$  kJ mol<sup>-1</sup>. Such low value of  $E_a$  suggests that the reorientational jumps of  $\text{NH}_3$  probably proceed through the translation–rotation coupling. Notwithstanding, one can observe the distinct changes between the neutron diffraction patterns before and after the  $T_C^h = 123.3$  K. All these facts suggest that the discovered phase transition is associated with a change of the crystal structure without a sudden change of the  $\text{NH}_3$  reorientational dynamics.

© 2011 Elsevier B.V. All rights reserved.

## 1. Introduction

At room temperature hexaamminecalcium perchlorate crystallizes in the cubic system (Fm  $\bar{3}m$  space group, no = 225) with unit cell parameter:  $a = 11.685$  Å and four molecules per unit cell [1] and is isostructural with many other hexaamminemetal(II) complexes, especially is very similar to  $[\text{Mg}(\text{NH}_3)_6](\text{ClO}_4)_2$  [2–4].  $[\text{Ca}(\text{NH}_3)_6](\text{ClO}_4)_2$  has between 95 and 295 K one solid phase transition at  $T_C^h = 123.3$  K (on heating) and at  $T_C^c = 122.0$  K (on cooling). The presence of ca. 1.3 K hysteresis of the phase transition temperature at  $T_C$  and the heat flow anomaly sharpness suggests that the detected phase transition is a first-order one. According to Fourier transform middle infrared spectra (FT-MIR) measurements, the observed phase transition is very probably associated with the

change of the crystal structure [1] We did not observe broadening of bands connected with  $\text{ClO}_4^-$  anions with increasing temperature. However, splitting of some bands was clearly visible [1].

Melting processes and thermal decompositions of  $[\text{Ca}(\text{NH}_3)_6](\text{ClO}_4)_2$  were studied by us using thermal gravimetry analysis (TGA) and differential scanning calorimetry (DSC) [5]. The gaseous products of the title compound thermal decomposition were on-line identified by a quadruple mass spectrometer (QMS). Among others the TGA/DSC/QMS results inform us that deamination process begins only just at ca. 340 K and finish fully at ca. 601 K [5].

The aim of the present study is to find connections between the previously recorded phase transition [5] with eventually changes of the rate of stochastic reorientational motions of the  $\text{NH}_3$  ligands or/and with a change of the crystal structure, by means of Fourier transform far infrared spectroscopy (FT-FIR), inelastic/quasi-elastic incoherent neutron scattering (IINS/QENS) and neutron powder diffraction (NPD) methods. The first two above mentioned meth-

\* Corresponding author. Tel.: +48 12 663 2265; fax: +48 12 634 0515.  
E-mail address: [hetmancz@chemia.uj.edu.pl](mailto:hetmancz@chemia.uj.edu.pl) (Ł. Hetmańczyk).

ods, beside information about vibrational dynamic, can inform us also about fast reorientational molecular motions, if the reorientational correlation times  $\tau_R$  are of an order:  $10^{-11}$ – $10^{-13}$  s.

## 2. Experimental

The sample of the title compound used in these measurements was synthesized by us in exactly the same manner as the sample used in our previous measurements [5].

The incoherent, inelastic/quasi-elastic neutron scattering spectra were measured using the time-of-flight method in the NERA-PR spectrometer [6] at the high flux pulsed reactor IBR-2, in Dubna (Russia) at temperatures  $T=20, 110, 131$  and  $220$  K. The sample of mass ca. 8 g was mounted at room temperature into a thin-walled, flat aluminium container, which was placed in a top-loaded cryostat cooled using a helium refrigerator. The neutron flux passed through  $5 \times 15 = 75 \text{ cm}^2$  sample area. The neutron transmission was ca. 72.5%. The temperature of the sample could be changed within the range 20–300 K and stabilized with  $\pm 0.5$  K accuracy at any chosen value. The energy resolution of the NERA-PR spectrometer amounts to ca. 3% for the IINS spectra in the range of  $1000$ – $100 \text{ cm}^{-1}$ . The energy of incoming neutrons was equal to  $4.64 \text{ meV}$  (neutrons were monochromatized using Bragg scattering from pyrolytic graphite). The spectral width of peak with maximum at ca.  $4.2 \text{ \AA}$  equals to ca.  $3.4 \text{ cm}^{-1}$ . The IINS measurements were made for several scattering angles. The final IINS spectra were obtained by summing up the data taken from all 15 detectors covering scattering angles from  $20^\circ$  to  $160^\circ$ . The quantitative analysis of the QENS spectra was performed for average scattering angle. Each spectrum was registered with good statistic (exposition time was approximately 10 h per one spectrum). The obtained spectra were corrected for the sample holder (Al) scattering and also the linear background coming from fast neutrons was subtracted. The data were not corrected for multi-scattering because of the small thickness of the sample. The registered QENS spectra show an asymmetry on the right side due to beryllium filters cut-off edge. Neutron powder diffraction (NPD) patterns were measured simultaneously with incoherent, inelastic/quasielastic neutron scattering (IINS/QENS) spectra. In the case of the NPD, different scattering angles were used to record the selected lattice spacing  $d_{hkl}$  ranges at an appropriate resolution. It should be emphasized that, because the examined compound contained ca. 50% of hydrogen atoms, the NPD patterns were recorded against a relatively high incoherent background, due to incoherent scattering cross-section of hydrogen atoms. For this reason, their interpretation is only qualitative, nevertheless it was very useful for identification of the particular phases.

The far infrared (FT-FIR) absorption measurements were performed using a Bruker 70v vacuum Fourier transform spectrometer. The transmission spectra were collected with a resolution of  $2 \text{ cm}^{-1}$  and with 64 scans per each spectrum. The FT-FIR spectra ( $600$ – $80 \text{ cm}^{-1}$ ) were collected for sample suspended in apiezon N grease and placed on polyethylene (PE) disc. Temperature measurement was carried out using Advanced Research System cryostat DE-202A and water cooled helium compressor ARS-2HW working in a closed cycle manner. The sample was loaded at room temperature and measurements were performed on cooling down to 8 K. The desired temperature was measured with accuracy of  $\pm 0.1$  K and stabilized for ca. 3 min before the measurements were taken. The LakeShore 3315 temperature controller equipped with diode sensor was used to control the temperature. The cooling rate between desired temperature was ca.  $3 \text{ K min}^{-1}$ . The PE windows were used in a cryostat in the case of FT-FIR measurements.

Fourier transform Raman scattering (FT-RS) measurements were performed at room temperature with a Bio-Rad spectrometer, resolution  $4 \text{ cm}^{-1}$ . The incident radiation ( $\lambda = 1064 \text{ nm}$ ) was from the Neodymium laser YAG Spectra-Physics.

## 3. Results and discussion

### 3.1. Vibrational spectrum

Experimental infrared spectra and phonon density of states function  $G(\nu)$  from IINS at 20 K and Raman spectra (FT-RS) at 295 K of  $[\text{Ca}(\text{NH}_3)_6](\text{ClO}_4)_2$  are presented in Fig. 1. Table 1 contains the bands frequencies of the Raman scattering and infrared absorption spectra obtained at the lowest temperature of the measurements and compared with the bands frequencies of the phonon density function  $G(\nu)$ . The assignments of these vibrations were proposed by comparing their frequencies with the literature data for several similar ionic amminemetal(II) complexes [7–9]. All characteristic bands frequencies of the internal vibrations of  $\text{NH}_3$  and  $\text{ClO}_4^-$  were found and some of the bands connected with stretching of Ca–N and bending of the N–Ca–N bonds were observed, too.

According to the group theory, unperturbed  $\text{ClO}_4^-$  anion with  $T_d$  symmetry generates four vibrational modes:  $\nu_1 = \nu_s(\text{ClO})A_1$  at ca.  $930 \text{ cm}^{-1}$ ,  $\nu_2 = \delta_d(\text{OCIO})E$  at ca.  $460 \text{ cm}^{-1}$ ,  $\nu_3 = \nu_{as}(\text{ClO})F_2$  at ca.

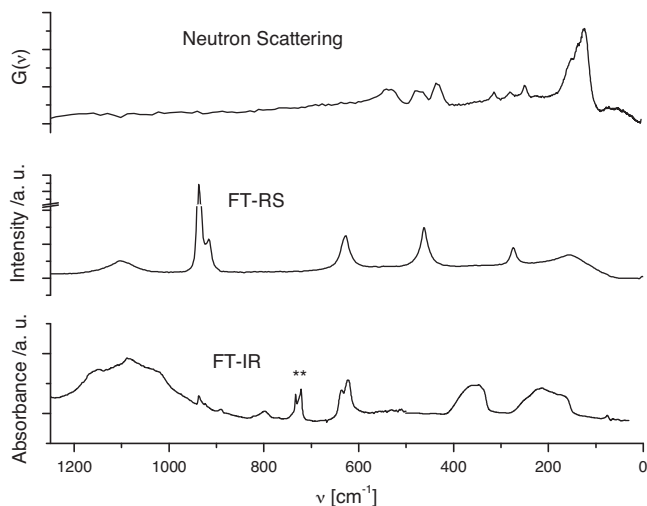


Fig. 1. Comparison of experimental far infrared (FT-FIR) spectrum, phonon density function  $G(\nu)$  calculated from IINS spectrum, both at 20 K, and Raman scattering (FT-RS) spectrum at 295 K for  $[\text{Ca}(\text{NH}_3)_6](\text{ClO}_4)_2$  (\*\* denotes bands of Nujol).

$1115 \text{ cm}^{-1}$  and  $\nu_4 = \delta_d(\text{OCIO})F_2$  at ca.  $630 \text{ cm}^{-1}$ . For an isolated  $\text{ClO}_4^-$  anion all these four modes are Raman active and only  $\nu_3$  and  $\nu_4$  are IR active. However, when the structure of the  $\text{ClO}_4^-$  anions is perturbed somehow, its degenerated vibrational modes may split and some of the inactive modes may be activated [10,11].

The proton-weighted phonon density of states function  $G(\nu)$  was calculated according to the formula (1) for double differential cross-section  $\sigma$  of neutrons scattered on protons in the sample [12]:

$$\frac{d^2\sigma}{d\Omega dE} = \frac{|\vec{k}_f|}{|\vec{k}_i|} \sum_p \frac{\sigma_{\text{inc},p}}{4\pi} \frac{\exp(-2W_p(\vec{Q}, \nu))}{1 - \exp(-h\nu/2k_B T)} \times G(\nu), \quad (1)$$

where  $\vec{k}_i$  and  $\vec{k}_f$  are the wave vectors of incident and scattered neutrons, respectively,  $\sigma_{\text{inc},p}$  is the incoherent scattering cross section,  $\exp(-2W_p(\vec{Q}, \nu))$  is so called the Debye–Waller factor. The neutron momentum transfer vector  $\vec{Q} = \vec{k}_i - \vec{k}_f$  scans Brillouin zones and  $k_B$  is the Boltzmann constant. The  $G(\nu)$  function, calculated in the one-phonon approximation from the time-of-flight IINS spectra of  $[\text{Ca}(\text{NH}_3)_6](\text{ClO}_4)_2$  against the neutron wavenumber scale for the lowest measurement temperature (at 20 K) is shown in Fig. 1. The

Table 1

The list of band positions of the phonon density function  $G(\nu)$  from IINS, infrared (FT-MIR) spectra at 20 K and Raman (FT-RS) spectra at 295 K of  $[\text{Ca}(\text{NH}_3)_6](\text{ClO}_4)_2$ .

Frequency ( $\text{cm}^{-1}$ )			Assignments	
	$G(\nu)$ at 20 K	IR at 20 K		RS at 295 K
		1149	$\nu_{as}(\text{ClO})F_2$	
		1088	$\nu_{as}(\text{ClO})F_2$	
		937	$\nu_s(\text{ClO})A_1$	
			916	$2\delta(\text{OCIO})E + A_1$
		798	$\rho_r(\text{NH}_3)F_{1u}$	
		637	$\delta_d(\text{OCIO})F_2$	
		622	$\delta_d(\text{OCIO})F_2$	
541		542	$\rho_r(\text{NH}_3)F_{2u}$	
477			$\nu_{as}(\text{CaN})F_{1u}$	
			463	$\delta_d(\text{OCIO})E$
437			$\nu(\text{CaN})E_g$	
314		344	$\delta_{as}(\text{NCaN})F_{2g}$	
281			$\nu(\text{CaN})F_{1u}$	
251			$\delta(\text{NCaN})F_{2g}$	
226		217	$\delta(\text{NCaN})F_{1u}$	
		176	$\nu_L(\text{Lattice})E_g$	
123		90	$\nu_L(\text{Lattice})F_{1u}$	
74			$\nu_L(\text{Lattice})F_{2g}$	
53			$\nu_L(\text{Lattice})F_{2g}$	

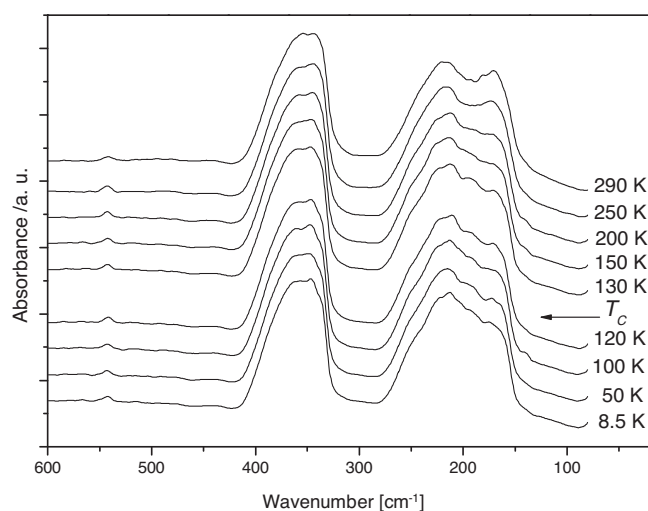


Fig. 2. Selected FT-FIR spectra in the frequency range of 600–80  $\text{cm}^{-1}$  at different temperatures (on cooling of  $[\text{Ca}(\text{NH}_3)_6](\text{ClO}_4)_2$ ).

intensity of the scattered neutrons depends on two factors. Firstly it depends on the displacement of atoms involved in vibrations (this factor is included in Debye–Waller expression) and secondly it depends on incoherent scattering length. Hence, due to a large incoherent cross section for hydrogen atoms, neutron spectroscopy is especially well situated in the studies of molecules containing hydrogen atoms. The scattering from the part of molecules containing hydrogen atoms dominates that from the rest atoms. It should be reminded here that in the  $G(\nu)$  spectrum, because there are no symmetry-dependent selection rules, contrary to the situation for infrared and Raman spectra, the bands connected with all molecular vibrations are allowed. The  $G(\nu)$  spectra obtained for the low temperature phase at temperature 20 K show some sharp and separate peaks characteristic for an ordered phase. However, a marked broadening of all these bands indicates the existence of  $\text{NH}_3$  orientational disorder present even at lowest temperatures. The  $G(\nu)$  spectra obtained at 110, 131 and 220 K are very diffuse, because of a large dynamical disorder connected with the fast molecular reorientations, especially of  $\text{NH}_3$  molecules.

### 3.2. Molecular motions and phase transition

#### 3.2.1. Far infrared absorption spectra vs. temperature

Fig. 2 shows the FT-FIR spectra of  $[\text{Ca}(\text{NH}_3)_6](\text{ClO}_4)_2$ , within the wavenumber range 600–80  $\text{cm}^{-1}$  registered during the cooling of the sample from 295 to 8.5 K. The spectrum at room temperature contains three bands. Two of them: at 174  $\text{cm}^{-1}$  and at 217  $\text{cm}^{-1}$  are connected with the  $\nu_L$  lattice vibration modes, and that at 344  $\text{cm}^{-1}$  is connected with the  $\delta_{\text{as}}(\text{NCaN})F_{1u}$  mode of internal vibration of  $[\text{Ca}(\text{NH}_3)_6]^{2+}$  octahedral cation. Some interesting changes can be noticed in the region of lattice vibration. During the cooling of the sample the shape of this band changes. In the high temperature phase one can see two separate bands of almost the same intensity. When the temperature drops, the intensity of the band at 174  $\text{cm}^{-1}$  decreases and a new band between the two observed previously appears at ca. 190  $\text{cm}^{-1}$ . However, the width of the band does not change. Such a behavior may suggest the change of the crystal structure. It is not connected with changes in molecular reorientation. In the FIR region we did not registered bands connected with  $\text{ClO}_4^-$  anions and hence it was impossible to draw any conclusions concerning the behavior (narrowing or splitting of bands) of this ion in the vicinity of the phase transition.

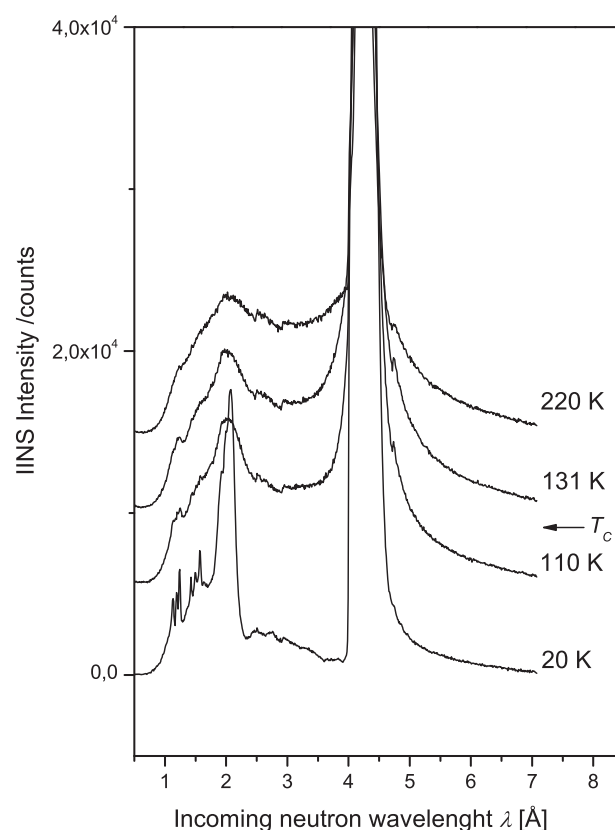


Fig. 3. Temperature dependence of the IINS/QENS spectra of  $[\text{Ca}(\text{NH}_3)_6](\text{ClO}_4)_2$ .

#### 3.2.2. Inelastic and quasielastic neutron scattering vs. temperature

The time-of-flight IINS spectra of  $[\text{Ca}(\text{NH}_3)_6](\text{ClO}_4)_2$  as a function of neutron wavelength, registered simultaneously with the NPD patterns, for four temperatures of measurements are presented in Fig. 3. In the IINS spectra presented in Fig. 3, one can also observe a distinct difference between the widths of the peaks (centered at a wavelength of 4.2 Å) registered at 20 and 110 K. The peak, registered at 110 K and also at higher temperatures, shows a distinct broadening, that is typical for the dynamics in orientationally disordered crystals (ODIC) [13]. Particularly, a quasielastic neutron scattering (QENS) component is very clearly visible left to the elastic peak. Given the energy resolution of the NERA spectrometer, this implies the occurrence of fast stochastic molecular motions. We conclude that these are picoseconds reorientational  $120^\circ$  jumps of  $\text{NH}_3$  molecules around their 3-fold axis of symmetry. This fact confirms that at the phase transition at  $T_C$  to the low temperature phase, the  $\text{NH}_3$  ligands do not change the rate of their reorientational jumps, which is fully compatible with the results obtained by our infrared spectroscopy measurements.

It is convenient to analyze the quasielastic neutron scattering data in terms of an elastic incoherent structure factor EISF defined as follows [14,15]:

$$\text{EISF} = \frac{I_{el}(Q)}{I_{el}(Q) + I_{qel}(Q)}, \quad (2)$$

where  $I_{el}(Q)$  and  $I_{qel}(Q)$  are intensities of elastic and quasielastic component, respectively, determined at a momentum transfer  $Q = (4\pi/\lambda) \sin(\theta)$ . The EISF gives information on the geometry of motion, especially of those parts of the molecules which contain the hydrogen atoms due to high incoherent scattering cross section. Moreover, the EISF parameter calculated for chosen  $Q$  value is temperature independent (assuming that during lowering of tem-

perature and especially after the phase transitions the distance of proton from the axis of rotation does not change).

For instantaneous angular jumps around the  $n$ -fold axis, the scattering law  $S(Q, \omega)$  for powder sample consists of two components and can be expressed by the following formula:

$$S(Q, \omega) = y_0 + N \cdot [\text{EISF}(Q) \cdot \delta(\omega) + (1 - \text{EISF}(Q)) \cdot L(\omega, \Gamma)], \quad (3)$$

where  $y_0$  is the linear background,  $N$  is the normalization factor,  $\delta(\omega)$  represents the elastic part and  $L(\omega, \Gamma)$  is the Lorentzian function of the type:

$$L(\omega, \Gamma) = \frac{1}{\pi} \frac{\Gamma}{\Gamma^2 + \omega^2}, \quad (4)$$

which represents quasielastic broadening. The width  $\Gamma$  (HWHM – half width at half maximum) has two major properties: firstly, it is inversely proportional to the mean time  $\tau$  between instantaneous jumps and secondly, it is independent of the scattering vector  $Q$ . Eq. (3) convoluted with the instrumental resolution function (see Eq. (5)) was fitted to the experimental data. The parameters:  $y_0$ ,  $N$ , EISF and  $\Gamma$  were determined by best fit using the least squares method. The data for a polycrystalline sample, as stated above, were registered for the chosen momentum transfer  $Q = 2.1 \text{ \AA}^{-1}$  (average scattering angle equals to  $44^\circ$ ). The spectrum registered at the lowest temperature (20 K) was taken as an resolution function, because no broadening of it was observed. The quasielastic broadening starts appearing with the resolution available at about 110 K. The resolution component was described by the Gaussian function:

$$\text{RES}(\omega) = A \cdot \exp\left(-\left(\frac{\omega - \omega_c}{\Delta}\right)^2\right), \quad (5)$$

where  $A$  is intensity (normalization),  $\omega_c = 4.64 \text{ meV}$  is the energy of incoming neutrons (neutrons were monochromatized using Bragg scattering from pyrolytic graphite),  $\Delta$  is the energy resolution of the TOF spectrometer. The parameters:  $A$ ,  $\omega_c$  and  $\Delta$  were fitted by the least square method.

Fig. 4 shows the quality of the total fit (solid line) with the quasielastic component (dotted line) and the resolution component (dashed line) for momentum transfer  $Q = 2.1 \text{ \AA}^{-1}$ . The fitting procedure was applied only to the part of the experimental points due to the Be filter cut-off edge. The analysis of EISF was performed at a temperature of 220 K. The theoretical EISF for  $120^\circ$  jumps model of all  $\text{NH}_3$  is given by:

$$\text{EISF}(Q) = \frac{1}{3} \cdot \left[ 1 + \frac{2 \cdot \sin(Q \cdot r \cdot \sqrt{3})}{Q \cdot r \cdot \sqrt{3}} \right]. \quad (6)$$

The  $r = 0.73 \text{ \AA}$  parameter denotes proton distance to the 3-fold rotation axis. One can see quite good agreement between elastic incoherent structure factor value (EISF = 0.463) calculated according to Eq. (6) and the experimentally one (EISF = 0.476(3)) determined from Eq. (3). Thus, one can conclude that the motion of  $\text{NH}_3$  groups in  $[\text{Ca}(\text{NH}_3)_6](\text{ClO}_4)_2$  can be well described by a simple model of  $120^\circ$  instantaneous jumps around the 3-fold axis. All the protons of the  $\text{NH}_3$  ligands performed jumps between their equivalent sites on a circle separated by  $120^\circ$  within picoseconds time scale. The  $\text{NH}_3$  groups perform fast stochastic reorientation in the temperature range of 110–290 K. This motion is not strongly affected by the phase transition detected by means of DSC method. Phases above 110 K are dynamically orientationally disordered crystals (ODIC). One can see broadening of the QENS spectra as well as broadening and diffused character of the peaks in the  $G(\nu)$  phonon density of states function.

Determination of the QENS width (Lorentzian part,  $\Gamma$ ) as a function of temperature allows one to calculate the activation energy  $E_a(\text{NH}_3)$  for the reorientational motions of  $\text{NH}_3$  molecules. This is

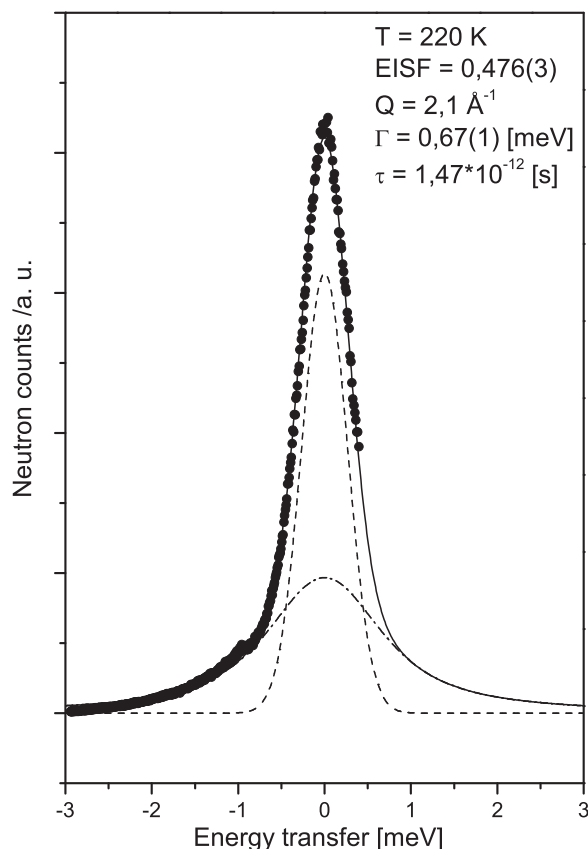


Fig. 4. Example of fitting the  $120^\circ$  jumps model to the QENS experimental spectrum for  $T = 220 \text{ K}$  (●, experimental points; —, elastic (resolution) component; ·····, quasielastic component).

the thermally activated process and can be well described by the Arrhenius law:

$$\Gamma(T) = A_0 \exp\left(\frac{-E_a}{RT}\right), \quad (7)$$

where  $A_0$  is a pre-exponential factor,  $R = N_A \cdot k_B$  is the gas constant,  $N_A$  is Avogadro's number and  $k_B$  is Boltzmann constant.

Fig. 5 shows an Arrhenius plot of  $2\Gamma$  vs.  $1000/T$ . The lines presented in Fig. 5 represent the best linear fit to experimental points.

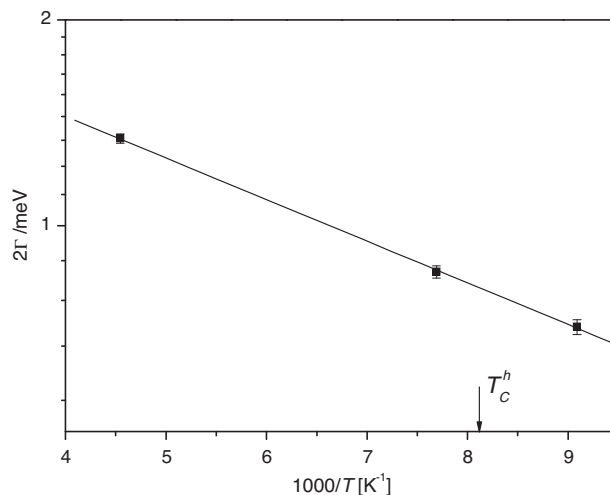


Fig. 5. FWHM of the QENS component ( $2\Gamma$ ) vs.  $1000/T$ . The symbol (■) denotes  $2\Gamma$  obtained for selected momentum transfer  $Q$ . The vertical lines denote experimental errors.

The estimated single (mean) activation energy for both phases (high at 220 and 131 K and the low at 110 K) equals to 12.1 meV ( $1.2 \text{ kJ mol}^{-1}$ ). The arrow indicates phase transition temperature determined by the DSC method.

Similar values of activation energy for  $120^\circ$  jumps around 3-fold axis around M–N bond were observed, for example, in other ionic coordination compounds:  $[\text{Mg}(\text{NH}_3)_6](\text{ClO}_4)_2$  [16,17] and  $[\text{Zn}(\text{NH}_3)_4](\text{ClO}_4)_2$  [18]. Namely, the experimentally determined activation energy value  $E_a(120^\circ)$  equals to 15.5 meV ( $1.5 \text{ kJ mol}^{-1}$ ) for the high temperature phase and  $34.2 \text{ meV}$  ( $3.3 \text{ kJ mol}^{-1}$ ) for the intermediate and low temperature phases of  $[\text{Mg}(\text{NH}_3)_6](\text{ClO}_4)_2$ . Similarly,  $E_a(120^\circ)$  value equals to  $25.9 \text{ meV}$  ( $2.5 \text{ kJ mol}^{-1}$ ) for high and intermediate temperature phases and  $17.6 \text{ meV}$  ( $1.7 \text{ kJ mol}^{-1}$ ) for the low temperature phase of  $[\text{Zn}(\text{NH}_3)_4](\text{ClO}_4)_2$ .

The mean time  $\tau$  between jumps, calculated according to the following relation:  $\tau = 3\hbar/2\Gamma$  decreases with temperature increasing. It changes from  $2.8 \times 10^{-12} \text{ s}$  at 110 K through  $2.3 \times 10^{-12} \text{ s}$  at 131 K to  $1.5 \times 10^{-12} \text{ s}$  at 220 K. The peak, registered at 110 K, and also those at higher temperatures, show a distinct broadening, which is typical for dynamically, orientationally disordered crystals (ODIC). The low values of the activation energies suggest that the reorientation of the  $\text{NH}_3$  ligands proceeds through the translation–rotation coupling [19,20], which means that the real barrier to the rotation of the  $\text{NH}_3$  is not constant but fluctuating. This is a very common feature among all hexaamminemetal(II) and hexaamminemetal(III) salts [21–23]. There is no evidence that  $\text{NH}_3$  jumps are strongly perturbed at least at the  $T_C$  phase transition. Ammonia molecules perform  $120^\circ$  jumps on a picoseconds time scale in all phases and do not suddenly change the jump rate of their reorientational motion. Such type of motion was earlier observed in many hexaamminemetal(II) compounds (see, for instance, Ref. [24] and the papers cited therein).

One should bear in mind that the resolution of the TOF spectrometer does not allow investigating the too fast motion. For high temperatures the QENS broadening, connected with very fast motion, is too big ( $\tau$  is too small) in comparison with the resolution of the TOF spectrometer and the wings of the quasielastic peak are hidden in the background. The proposed model of reorientation of  $\text{NH}_3$  molecules is rather simple. One cannot exclude the possibility of a very complex motion (for example anisotropic of the whole complex cation) which was not taken into account in performed QENS analysis. This complex motion can also give some contribution to the QENS broadening but it is usually slower than  $\text{NH}_3$  jumps and is beyond the time scale window of this method. On the other hand, rather a poor resolution function does not allow investigating too slow motion (because the quasielastic component is hidden in the resolution function).

### 3.3. Neutron powder diffraction

The neutron diffraction patterns (NPD) for polycrystalline  $[\text{Ca}(\text{NH}_3)_6](\text{ClO}_4)_2$ , registered during the sample heating up at four selected temperatures of measurement: 20, 110, 131, 220 K for scattering angle:  $2\theta = 69.1^\circ$ . We can see some important differences between the NPD patterns obtained for two crystalline phases: high and low temperature phase. Fig. 6 presents differences between the NPD patterns registered at 131 (high temperature phase – I) and 110 K (low temperature phase – II) for scattering angles  $2\theta = 69.1^\circ$ . Bars at the top of the figure denote  $d_{hkl}$  spacing calculated for crystal structure determined from single X-ray measurements. One can observe appearing of a new reflection peak at  $4.0 \text{ \AA}$  in 110 K at the vicinity of  $T_C$ . This suggests that during the phase transition crystal structure change takes place. The NPD patterns can be evaluated only qualitatively. It does not allow to relate structure (an average position or orientation of

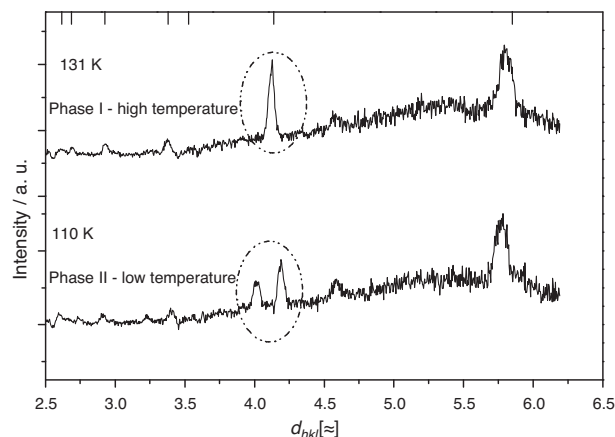


Fig. 6. Differences between the NPD patterns of  $[\text{Ca}(\text{NH}_3)_6](\text{ClO}_4)_2$  registered at 131 and 110 K, for scattering angle  $2\theta = 69.1^\circ$ .

atoms) with dynamics. However, they provide useful and important results.

## 4. Conclusions

1. Temperature dependence of far infrared spectra suggests that the observed phase transition is probably associated with a change of the crystal structure. The lack of simultaneous abrupt narrowing of some broad infrared bands suggests an existence of fast molecular reorientational motions, which do not change their character in the wide temperature range.
2. The  $\text{NH}_3$  ligands in  $[\text{Ca}(\text{NH}_3)_6](\text{ClO}_4)_2$  perform fast stochastic reorientation, which can be well described by a simple model of instantaneous  $120^\circ$  proton jumps around the 3-fold Ca–N axis, within the picoseconds correlation time scale. This motion is not affected by the phase transition detected by means of DSC method at  $T_C \sim 123 \text{ K}$ . The high temperature phase is dynamically orientationally disordered crystal phase. One can see broadening of the QENS spectra as well as broadening and diffused character of the peaks in the phonon density of states function  $G(\nu)$ .
3. The estimated from QENS measurements mean for high and low temperature phases activation energy for  $\text{NH}_3$  ligands stochastic reorientation equals to  $1.2 \text{ kJ mol}^{-1}$ . The low value of the activation energy suggests that the reorientation of the  $\text{NH}_3$  ligands proceeds through the translation–rotation coupling.
4. The neutron diffraction patterns registered at 220 and 131 K (high temperature phase I) are different than this obtained at 110 K (low temperature phase II). Changes observed in diffraction patterns of  $[\text{Ca}(\text{NH}_3)_6](\text{ClO}_4)_2$  suggest that the phase transition at  $T_C \approx 123 \text{ K}$  is associated with a change of the crystal structure.

## Acknowledgments

The far infrared research was carried out with the equipment purchased thanks to the financial support of the European Regional Development Fund in the framework of the Polish Innovation Economy Operational Program (contract no. POIG.02.01.00-12-023/08). We are very grateful to Dr hab. A. Weselucha-Birczyńska from the Faculty of Chemistry of the Jagiellonian University for registering FT-RS spectrum of title compound at room temperature.

## References

- [1] J. Hetmańczyk, A. Migdał-Mikuli, Ł. Hetmańczyk, Ann. Pol. Chem. Soc. (2007) 358–361, ISBN: 978-83-922424r-r7-5.

- [2] R.W.G. Wyckoff, *Crystal Structure*, vol. 3, second edition, Interscience Publishers, New York, 1965.
- [3] A. Migdał-Mikuli, E. Mikuli, M. Rachwalska, S. Hodorowicz, *Phys. Status Solidi A* 47 (1978) 57–64.
- [4] S. Hodorowicz, M. Ciechanowicz-Rutkowska, J.M. Janik, J.A. Janik, *Phys. Status Solidi A* 43 (1977) 53–57.
- [5] A. Migdał-Mikuli, J. Hetmańczyk, *J. Therm. Anal. Calorim.* 91 (2) (2008) 529–534.
- [6] I. Natkaniec, S.I. Bragin, J. Brańkowski, J. Mayer, *Proceedings ICANS XII Meeting*, Abington 1993. RAL Report 94-025, vol. I, 1994, p. 89.
- [7] J. Fujita, K. Nakamoto, M. Kobayashi, *J. Am. Chem. Soc.* 78 (1956) 3295.
- [8] A. Migdał-Mikuli, E. Mikuli, M. Barańska, Ł. Hetmańczyk, *Chem. Phys. Lett.* 381 (2003) 329–334.
- [9] E. Mikuli, A. Migdał-Mikuli, N. Górska, S. Wróbel, J. Ściesiński, E. Ściesińska, *J. Mol. Struct.* 651–653C (2003) 519–524.
- [10] Y.H. Zhang, C.K. Chan, *J. Phys. Chem. A* 107 (2003) 5956–5962.
- [11] L.-J. Zhao, Y.-H. Zhang, L.-Y. Wang, Y.-A. Hu, F. Ding, *Phys. Chem. Chem. Phys.* 7 (2005) 2723–2730.
- [12] S.W. Lovesey, *Theory of Neutron Scattering from Condensed Matter*, Clarendon Press, Oxford, 1984.
- [13] S.W. Lovesey, T. Springer (Eds.), *Topics in Current Physics*, vol. 3, Springer-Verlag, Berlin, 1977.
- [14] S. Mitra, R. Mukhopadhyay, *Molecular dynamics using quasielastic neutron scattering technique*, *Curr. Sci.* 84 (2003) 653–662.
- [15] C. Nöldeke, B. Asmussen, W. Press, H. Buttner, G. Kearley, *Chem. Phys.* 289 (2003) 275–280.
- [16] E. Mikuli, *Dynamika molekularna związków typu  $[\text{Me}(\text{NH}_3)_6]\text{X}_2$  i  $[\text{Me}(\text{H}_2\text{O})_6]\text{X}_2$* , Rozprawy habilitacyjne UJ nr 300, Kraków, 1995.
- [17] J.A. Janik, J.M. Janik, A. Migdał-Mikuli, E. Mikuli, K. Otnes, I.I. Svare, *Physica B* 97 (1979) 47–56.
- [18] A. Migdał-Mikuli, K. Holderna-Natkaniec, E. Mikuli, Ł. Hetmańczyk, I. Natkaniec, *Chem. Phys.* 335 (2007) 187–193.
- [19] P. Schiebel, W. Prandl, *Z. Phys. B* 104 (1997) 137–145.
- [20] K.H. Michel, J. Naudts, *J. Chem. Phys.* 67 (1977) 547–558.
- [21] J.A. Janik, J.M. Janik, A. Migdał-Mikuli, E. Mikuli, K. Otnes, *Physica B* 138 (1986) 280–286.
- [22] A. Migdał-Mikuli, E. Mikuli, N. Górska, A. Kowalska, J. Ulański, *J. Solid State Chem.* 177 (2004) 2733–2739.
- [23] E. Mikuli, N. Górska, S. Wróbel, J. Ściesiński, E. Ściesińska, *J. Mol. Struct.* 692 (2004) 231–236.
- [24] J.M. Janik, J.A. Janik, A. Migdał-Mikuli, E. Mikuli, K. Otnes, *Physica B* 168 (1991) 45–52.